



# Tumor-Selective Altered Glycosylation and Functional Attenuation of CD73 in Human Hepatocellular Carcinoma

Karel P. Alcedo,<sup>1</sup> Andres Guerrero,<sup>2</sup> Venkatesha Basrur,<sup>3</sup> Dong Fu <sup>1</sup>, Monea L. Richardson,<sup>1</sup> Joshua S. McLane,<sup>1</sup> Chih-Chiang Tsou,<sup>4</sup> Alexey I. Nesvizhskii,<sup>3,4</sup> Theodore H. Welling,<sup>5</sup> Carlito B. Lebrilla,<sup>2</sup> Carol A. Otey,<sup>1</sup> Hong Jin Kim,<sup>6</sup> M. Bishr Omary,<sup>7-9</sup> and Natasha T. Snider <sup>1</sup>

CD73, a cell-surface *N*-linked glycoprotein that produces extracellular adenosine, is a novel target for cancer immunotherapy. Although anti-CD73 antibodies have entered clinical development, CD73 has both protumor and antitumor functions, depending on the target cell and tumor type. The aim of this study was to characterize CD73 regulation in human hepatocellular carcinoma (HCC). We examined CD73 expression, localization, and activity using molecular, biochemical, and cellular analyses on primary HCC surgical specimens, coupled with mechanistic studies in HCC cells. We analyzed CD73 glycan signatures and global alterations in transcripts encoding other *N*-linked glycoproteins by using mass spectrometry glycomics and RNA sequencing (RNAseq), respectively. CD73 was expressed on tumor hepatocytes where it exhibited abnormal *N*-linked glycosylation, independent of HCC etiology, tumor stage, or fibrosis presence. Aberrant glycosylation of tumor-associated CD73 resulted in a 3-fold decrease in 5'-nucleotidase activity ( $P < 0.0001$ ). Biochemically, tumor-associated CD73 was deficient in hybrid and complex glycans specifically on residues N311 and N333 located in the C-terminal catalytic domain. Blocking N311/N333 glycosylation by site-directed mutagenesis produced CD73 with significantly decreased 5'-nucleotidase activity *in vitro*, similar to the primary tumors. Glycosylation-deficient CD73 partially colocalized with the Golgi structural protein GM130, which was strongly induced in HCC tumors. RNAseq analysis further revealed that *N*-linked glycoprotein-encoding genes represented the largest category of differentially expressed genes between HCC tumor and adjacent tissue. **Conclusion:** We provide the first detailed characterization of CD73 glycosylation in normal and tumor tissue, revealing a novel mechanism that leads to the functional suppression of CD73 in human HCC tumor cells. The present findings have translational implications for therapeutic candidate antibodies targeting cell-surface CD73 in solid tumors and small-molecule adenosine receptor agonists that are in clinical development for HCC. (*Hepatology Communications* 2019;3:1400-1414).

**E**cto-5'-nucleotidase (CD73) is the major enzyme that dephosphorylates extracellular adenosine 5'-monophosphate (AMP) to produce adenosine. CD73 activity is ubiquitous in mammalian systems and regulates purine salvage and purinergic signaling

in tissue homeostasis, inflammation, fibrosis, and cancer.<sup>(1,2)</sup> CD73-generated adenosine can suppress antitumor T-cell responses, thereby promoting the progression of breast, skin, ovarian, and prostate cancer in animal models.<sup>(3)</sup> Several anti-CD73 inhibitory antibodies

*Abbreviations:* A<sub>3</sub>AR, adenosine A<sub>3</sub> receptor; AMP, adenosine monophosphate; ANOVA, analysis of variance; CD, clusters of differentiation; CD73, ecto-5'-nucleotidase; CF102, 2-chloro-N(6)-(3-iodobenzyl)adenosine-5'-N-methyluronamide or Namodenoson; DAPI, 4',6-diamidino-2-phenylindole; EndoH, endoglycosidase H; eNPP2, ectonucleotide pyrophosphatase/phosphodiesterase 2 gene; eNTPD8, ectonucleoside triphosphate diphosphohydrolase 8; ER, endoplasmic reticulum; HCC, hepatocellular carcinoma; K, keratin; LC, liquid chromatography; MS, mass spectrometry; NCBI, National Center for Biotechnology Information; NT5E, ecto-5'-nucleotidase; OG, n-octylglucoside; PBS, phosphate-buffered saline; PNGase F, peptide:N-glycosidase F; RNAseq, RNA sequencing; SDS-PAGE, sodium dodecyl sulfate-polyacrylamide gel electrophoresis; UM, University of Michigan; UNC, University of North Carolina at Chapel Hill; Vti1, v-SNARE; WT, wild type.

Received May 30, 2019; accepted July 7, 2019.

Additional Supporting Information may be found at [onlinelibrary.wiley.com/doi/10.1002/hep4.1410/supinfo](https://onlinelibrary.wiley.com/doi/10.1002/hep4.1410/supinfo).

Supported by the National Institutes of Health (grants DK110355 to N.T.S., DK47918 to M.B.O., GM094231 to A.N., and institutional grants DK034987 to the University of North Carolina [UNC] and DK034933 and CA210967 to the University of Michigan) and the UNC Cancer Cell Biology Training Grant Program (to K.P.A.) and the UNC Postbaccalaureate Research Education Program (to M.L.R.).

(MEDI9447, CPI-006, TJ004309, NZV930) are currently undergoing clinical testing for advanced solid tumors.<sup>(4,5)</sup> However, the role of CD73 in cancer is complex because CD73 activity is crucial for protecting endothelial and epithelial barrier functions,<sup>(6)</sup> particularly during hypoxic conditions,<sup>(7,8)</sup> and CD73 protects the epithelial integrity in well-differentiated early stage endometrial carcinoma, which is associated with better overall patient survival.<sup>(9)</sup> This clearly demonstrates that the role of CD73 in cancer is not uniform and warrants a critical mechanistic evaluation of CD73 regulation and function at multiple levels and in different cancer types.<sup>(6)</sup>

CD73 is a known regulator of hepatocyte injury<sup>(10,11)</sup> and fibrogenic responses in the liver,<sup>(12,13)</sup> but its functional regulation in liver cancer has not been investigated to date. Given the importance of CD73 as a novel target for cancer therapy and the significant disease burden of liver cancer,<sup>(14)</sup> the aim of the present study was to investigate the regulation and activity of CD73 protein in human hepatocellular carcinoma (HCC). CD73 is widely expressed in hepatobiliary malignancies, and aberrant intense cytoplasmic CD73 staining is a marker of invasive lesions in HCC.<sup>(15)</sup> The mechanisms behind the aberrant CD73 localization and whether it is enzymatically active are not known. Novel interventions for HCC

are critically needed, and modulation of adenosine signaling represents one potential strategy. Specifically, the adenosine A<sub>3</sub> receptor (A<sub>3</sub>AR) is highly expressed in HCC, and its activation by a selective agonist (2-chloro-N<sup>6</sup>-(3-iodobenzyl)adenosine-5'-N-methyluronamide [CF102 or Namodenoson]) has antitumor effects in a rat model of HCC.<sup>(16)</sup> CF102 recently completed phase II clinical testing and showed a favorable clinical safety profile and a positive signal of efficacy in patients with advanced HCC and severe liver dysfunction, justifying further testing in phase III trials.<sup>(17,18)</sup> In light of the important role of adenosine signaling as a clinical target in HCC, it is critical to understand how the activity of the major extracellular AMPase CD73 is regulated in HCC tumors.

As a glycosylphosphatidylinositol-anchored protein (GPI-AP), CD73 undergoes complex processing by the secretory pathway.<sup>(19)</sup> Proteins destined for this pathway undergo initial maturation in the endoplasmic reticulum (ER) followed by vesicular transport through the Golgi apparatus before being targeted to their ultimate destinations through the *trans*-Golgi network. A key regulatory step in the proper execution of this process is the sequential covalent modification of proteins with oligosaccharides linked by asparagine residues, termed *N*-linked glycosylation.<sup>(20)</sup> Alterations in the *N*-linked glycoproteome

© 2019 The Authors. *Hepatology Communications* published by Wiley Periodicals, Inc., on behalf of the American Association for the Study of Liver Diseases. This is an open access article under the terms of the Creative Commons Attribution-NonCommercial-NoDerivs License, which permits use and distribution in any medium, provided the original work is properly cited, the use is non-commercial and no modifications or adaptations are made.

View this article online at [wileyonlinelibrary.com](http://wileyonlinelibrary.com).

DOI 10.1002/hep4.1410

Potential conflict of interest: Dr. Welling consults for Bristol-Myers Squibb and received grants from Merck. The other authors have nothing to report.

## ARTICLE INFORMATION:

From the <sup>1</sup>Department of Cell Biology and Physiology, University of North Carolina at Chapel Hill, Chapel Hill, NC; <sup>2</sup>Department of Chemistry, University of California Davis, Davis, CA; <sup>3</sup>Department of Pathology; <sup>4</sup>Department of Computational Medicine and Bioinformatics, University of Michigan, Ann Arbor, MI; <sup>5</sup>Perlmutter Cancer Center and Department of Surgery, New York University Langone Health, New York, NY; <sup>6</sup>Department of Surgery, University of North Carolina at Chapel Hill, Chapel Hill, NC; <sup>7</sup>Department of Molecular and Integrative Physiology; <sup>8</sup>Department of Medicine, University of Michigan, Ann Arbor, MI; <sup>9</sup>Center for Advanced Biotechnology & Medicine, Rutgers University, Piscataway, NJ; Rutgers Biomedical Health Sciences, Newark, NJ.

## ADDRESS CORRESPONDENCE AND REPRINT REQUESTS TO:

Natasha Snider, Ph.D.  
University of North Carolina at Chapel Hill  
Department of Cell Biology and Physiology, 5340C MBRB  
111 Mason Farm Road

Chapel Hill, NC 27516  
E-mail: [ntsnider@med.unc.edu](mailto:ntsnider@med.unc.edu)  
Tel.: +1-919-962-6033

are hallmarks of many cancers, including HCC.<sup>(21)</sup> In this study, we reveal a novel glycosylation mechanism leading to the mislocalization and functional suppression of CD73 in HCC tumors. Our results illuminate specific regulatory mechanisms that may be exploited for targeted treatment to improve outcomes in patients with HCC.

## Materials and Methods

### ANTIBODIES AND REAGENTS

Mouse anti-Flag M2 clone (Sigma-Aldrich) and rabbit anti-CD73 clone HPA017357 (Atlas Antibodies) were used to detect tagged and untagged (endogenous) CD73, respectively. Mouse anti-CD73 clone AD2 (BD Biosciences) was used for immunoprecipitation of CD73. Mouse anti-CD73 clone IE9 (Santa Cruz Biotechnology) was used to costain with tight junction markers ZO1 (rabbit; Cell Signaling) and claudin-1 (rabbit; Thermo Fisher Scientific). Other antibodies used were rat anti-keratin (K)19 (Troma-III; Developmental Studies Hybridoma Bank); rabbit anti-tissue nonspecific alkaline phosphatase (TNAP; Abcam); and mouse monoclonal antibodies for Golgi marker proteins GM130, Vti1, STx6, and GS27 (BD Biosciences). Complementary DNA encoding human ecto-5'-nucleotidase (*NT5E*)-1 and *NT5E*-2 in pCMV6-Entry and control empty vector were purchased from Origene. Endoglycosidase H (EndoH) and peptide:N-glycosidase F (PNGase F) glycosidases were used with liver lysates as recommended by the manufacturer (New England Biolabs).

### HUMAN SPECIMENS

Surgical specimens were collected under approved human subjects protocols at the University of Michigan (UM) and the University of North Carolina at Chapel Hill (UNC). HCC surgical specimens that were collected at UM have been described.<sup>(22)</sup> Normal human liver specimens were from surgical resections of unaffected liver tissue collected during removal of colorectal cancer metastasis to the liver. An additional 27 liver-tumor pairs of HCC surgical specimens (23 of which were CD73 positive) were collected at UNC under an approved human subject protocol (clinical information provided in Supporting File S1).

### CELL CULTURE, TRANSFECTIONS, IMAGING, IMMUNOBLOTTING, AND QUANTITATIVE POLYMERASE CHAIN REACTION

Huh7 cells were obtained from the Japanese Collection of Research Bioresources and cultured in Dulbecco's modified Eagle's medium supplemented with 10% fetal bovine serum and 100 U/mL penicillin/streptomycin. PLC/PRF5 cells were from the American Type Culture Collection (ATCC; Manassas, VA) and cultured according to ATCC recommendations. Site-directed mutagenesis was performed using the QuikChange kit (Agilent Technologies). For immunofluorescence analysis, human tissues or cells were fixed in methanol at  $-20^{\circ}\text{C}$  for 10 minutes, washed 3 times in phosphate-buffered saline (PBS) and incubated in blocking solution (2.5% bovine serum albumin, 2% normal goat serum in PBS) for 1 hour at room temperature. Primary antibodies were diluted in blocking buffer and incubated overnight at  $4^{\circ}\text{C}$ . Following three PBS washes, the cells/tissues were incubated with Alexa Fluor-conjugated secondary antibodies diluted in blocking solution for 1 hour at room temperature followed by 4',6-diamidino-2-phenylindole (DAPI) incubation for 5 minutes and mounted in Fluoromount-G (SouthernBiotech, Birmingham, AL) overnight. Secondary antibodies alone served as negative controls. A Zeiss 880 confocal laser scanning microscope using a  $63\times$  (1.4 numerical aperture) oil immersion objective (Zeiss, Jena, Germany) was used for imaging.

### BIOCHEMICAL ASSAY OF CD73 EXPRESSION AND ACTIVITY

CD73 was extracted from cells or liver tissue in 50 mM *n*-octylglucoside (Sigma) in PBS (OG lysis buffer) with freshly added complete protease inhibitor cocktail (Roche) and shaking for 2 hours at  $4^{\circ}\text{C}$ , followed by centrifugation at  $20,000g$  for 20 minutes. Immunoprecipitation of CD73 from OG lysates was performed using Dynabeads protein G (Thermo Fisher Scientific) following the manufacturer's instructions. Measurement of 5'-nucleotidase activity was performed using a commercial kit (Diazyme) with OG liver lysates that were first normalized to 1 mg/mL total protein concentration. This assay is

based on a four-reaction sequence beginning with the enzymatic hydrolysis of 5'-inosine monophosphate (5'-IMP) to form inosine, which is subsequently converted to hypoxanthine by purine nucleoside phosphorylase. Xanthine oxidase converts hypoxanthine to uric acid and hydrogen peroxide ( $H_2O_2$ ).  $H_2O_2$  is then reacted with N-ethyl-N-(2-hydroxy-3-sulfopropyl)-3-methylaniline and 4- aminoantipyrine in the presence of peroxidase to generate a quinone dye, which is monitored in a kinetic manner. The specificity of the 5'-IMP-based assay for CD73 activity was originally described in multiple tissues<sup>(8)</sup> and specifically in the liver, using CD73<sup>-/-</sup> liver lysates.<sup>(11)</sup>

## MASS SPECTROMETRY ANALYSIS OF SITE-SPECIFIC CD73 GLYCOSYLATION AND DETERMINATION OF GLYCAN STRUCTURES

CD73 was immunodepleted from liver and tumor OG lysates and subjected to mass spectrometry (MS) analysis to determine site-specific glycosylation and glycan structures. The band corresponding to CD73 protein was excised and destained with 30% methanol for 4 hours. Following reduction (10 mM dithiothreitol) and alkylation (65 mM 2-chloroacetamide) of the cysteines, proteins were digested overnight with sequencing-grade modified trypsin (Promega). Resulting peptides were resolved on a nanocapillary reverse phase column (Acclaim PepMap C18, 2  $\mu$ m, 15 cm; Thermo Scientific, San Jose CA) using a 1% acetic acid/acetonitrile gradient at 300 nL/minute and were directly introduced into an Orbitrap Fusion tribrid MS (Thermo Scientific). MS1 scans were acquired at 60K resolution. Data-dependent high-energy C-trap dissociation MS/MS spectra were acquired with top-speed option (3 seconds) following each MS1 scan (relative capillary electrophoresis ~35%). Fragment (daughter) ion masses were measured in orbitrap (resolution of 15K). XX peptide identification and site-specific glycan structures were determined using the program GP Finder, as described.<sup>(23)</sup> To determine glycopeptide abundance, we used the summation of elution apex intensities of all MS1 isotope peaks. MS1 precursor features of glycopeptides were extracted by the feature detection algorithm described in DIA-Umpire.<sup>(24)</sup> Feature detection was restricted to +3, +4, and +5 charge states and 3-5

isotope peaks. For each liquid chromatography (LC)/MS run, the detected features with close precursor mass-to-charge ratio ( $\pm 20$  ppm) and charge state identical to the identified glycopeptides were considered as the candidate features for quantification. For the identified glycopeptides, the feature closest to the identified retention time was extracted. If a glycopeptide was only identified in other LC/MS runs, the most intense candidate feature within a 2-minute retention time range of the identified retention times from other LC/MS runs was extracted.

## RNA SEQUENCING ANALYSIS OF DIFFERENTIALLY EXPRESSED GENES IN ADJACENT NONTUMOR LIVER TISSUE AND HCC TUMOR TISSUE

Surgical tissues from two adjacent liver-tumor pairs were preserved in RNAlater. Tumor CD73 displayed shift in migration on sodium dodecyl sulfate-polyacrylamide gel electrophoresis (SDS-PAGE) in both specimens. RNA was extracted using the RNeasy kit (Qiagen) and used for sequencing analysis (all RNA integrity number values were >9). For the published dataset (GSE 33294), sequence read archive data files were obtained from the National Center for Biotechnology Information (NCBI) Gene Expression Omnibus repository and converted into fastq files. The quality of the raw reads data was determined using FastQC. The software package Tuxedo Suite was used for alignment, differential expression analysis, and postanalysis diagnostics. FastQC was used for a second round of quality control (postalignment) to ensure that only high quality data would be input to expression quantitation and differential expression analysis. We used Cufflinks/CuffDiff (version 2.1.1) for expression quantitation and differential expression analysis, using University of California Santa Cruz (UCSC) hg19.fa as the reference genome sequence and UCSC hg19.gtf as the reference transcriptome annotation. We identified genes and transcripts as being differentially expressed based on three criteria: test status, "OK"; false discovery rate, <0.05; and fold change,  $\geq 1.5$ . We annotated genes and isoforms with NCBI Entrez GeneIDs and text descriptions. We further annotated differentially expressed genes with gene ontology terms using NCBI annotation. We used DAVID (version 6.7) for enrichment analysis of the set of differentially expressed genes



to identify significantly enriched functional categories; these are presented in Supporting File S2.

## Results

### CD73 IS EXPRESSED IN MALIGNANT HEPATOCYTES AND EXHIBITS CYTOPLASMIC DISTRIBUTION IN HCC TUMORS

Using data from the PanCancer Atlas Consortium,<sup>(25)</sup> we determined that the CD73-encoding gene (*NT5E*)

did not correlate with a specific tumor immune subtype in HCC (Fig. 1A). However, aside from its functions in the immune system, CD73 is also a well-known regulator of epithelial cells,<sup>(6)</sup> including hepatocytes.<sup>(11)</sup> Therefore, we investigated CD73 protein expression and localization in nondiseased (normal) liver and HCC tumor and adjacent nontumor tissues. Immunofluorescence imaging revealed abundant CD73 expression in normal liver and in HCC (Fig. 1B). CD73 in HCC adjacent liver tissue and tumor tissue appeared largely intracellular (Fig. 1B). Costaining with the tight junction marker ZO1 revealed CD73 presence in the cytoplasm as well as the lumen of bile canaliculi in adjacent liver tissue

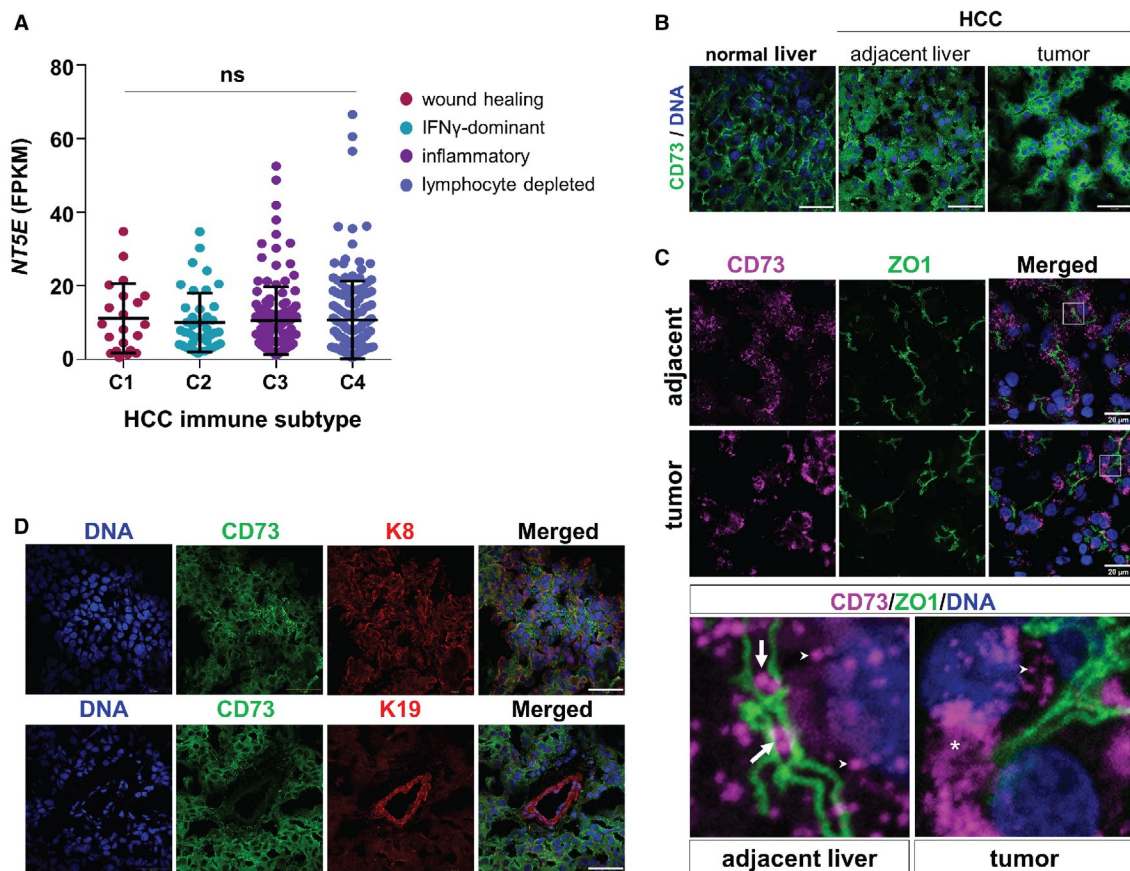


**FIG. 1.** CD73 is highly expressed in malignant hepatocytes in human HCC. (A) *NT5E* gene expression across tumors classified into the four major HCC immune subtypes: wound healing (C1), IFN $\gamma$ -dominant (C2), inflammatory (C3), and lymphocyte depleted (C4). Data were obtained from the PanCancer Atlas (one-way ANOVA; Tukey's multiple comparisons test). (B) Immunofluorescence analysis of CD73 (green) and DAPI-stained DNA (blue) in normal human liver tissue (left), HCC adjacent liver tissue (middle), and tumor tissue (right). Scale bars, 50  $\mu$ m. (C) Immunofluorescence analysis of CD73 (magenta), ZO1 (green), and DAPI-stained DNA (blue). Bottom panels represent boxed areas of the merged images, revealing cytoplasmic (asterisk) and punctate perinuclear (arrowhead) clustering of CD73 in HCC tumor and adjacent tissue. In adjacent liver tissue, CD73 was also localized in the lumen of the bile canaliculus (arrows). Scale bars, 20  $\mu$ m. (D) Immunofluorescence analysis of DAPI-stained DNA (blue), CD73 (green), and K8 and K19 (red), which mark hepatocytes and cholangiocytes, respectively. Scale bars, 50  $\mu$ m. Abbreviations: FPKM, fragments per kilobase of exon model per million reads mapped; IFN, interferon; ns, no statistical significance in expression between groups.

and primarily cytoplasmic and perinuclear distribution in the tumor tissue (Fig. 1C). To determine which epithelial cell types express CD73 in HCC tumors, we costained for the epithelial markers K8 and K19. CD73 is abundant in K8-positive but not K19-positive cells (Fig. 1D), suggesting that it is expressed primarily on malignant hepatocytes and absent from tumor cholangiocytes. By immunoblot analysis, we detected CD73 protein in all HCC cell lines we tested (Hep3B, Huh7, MHCC97, SNU-423, and SNU-449), while PLC/PRF/5 hepatoma cells were CD73 negative (Fig. 2A). Immunofluorescence analysis confirmed the lack of CD73 in the PLC/PRF5 cells (Fig. 2B) and revealed cytoplasmic and membranous distribution of CD73 in the Huh7 cells (Fig. 2B,C). Specifically, costaining with the tight junction markers ZO1 and claudin-1 showed CD73 localization within the lumen of small bile canaliculi-like structures (Fig. 2C, arrows) that Huh7 cells are known to form in culture<sup>(26)</sup> as well as the presence of CD73 in perinuclear puncta (Fig. 2C, arrowheads), similar to its distribution in the primary HCC tissues.

## TUMOR-SPECIFIC BIOCHEMICAL CHANGES ON CD73 CORRELATE WITH DECREASED 5'-NUCLEOTIDASE ACTIVITY

HCC typically develops in the context of cirrhosis, so we asked whether CD73 protein expression is different in the tumor versus the adjacent nontumor tissue. Immunoblot analysis (Fig. 3A) and quantification of band intensities from 23 CD73-positive HCC liver-tumor pairs (Fig. 3B; Supporting File S1) revealed heterogeneous expression of CD73. Of the 23 tumors, CD73 was increased in 11, unchanged in six, and decreased in six tumors, relative to adjacent liver. However, we also noted that in 13/23 (57%) of the CD73-positive liver-tumor pairs, CD73 from the tumor tissue migrated faster on SDS-PAGE gels compared to CD73 from adjacent nontumor liver, as shown by the representative immunoblot in Fig. 3C. Tumor-associated biochemical changes in CD73 were independent of HCC etiology, tumor stage, and

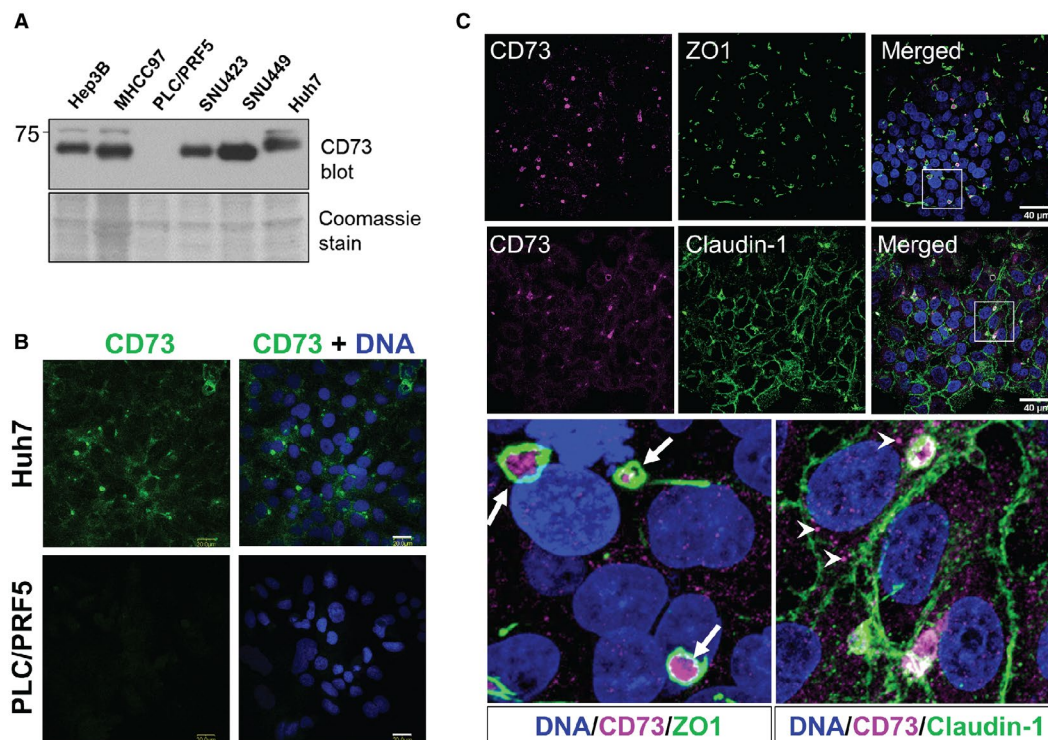


**FIG. 2.** CD73 is endogenously expressed in human HCC cell lines and exhibits membrane and cytoplasmic expression. (A) CD73 immunoblot and Coomassie stain (loading control) in HCC cell lines. (B) Immunofluorescence staining of CD73 (green) and DNA (blue) in Huh7 (CD73-positive) and PLC/PRF5 (CD73-negative) cell lines. Scale bars, 20 μm. (C) Immunofluorescence analysis of CD73 (magenta), ZO1 or claudin-1 (green; as labeled in panels), and DAPI-stained DNA (blue) in Huh7 cells. Bottom panels represent boxed areas of the merged images, revealing membrane (arrows) and punctate cytoplasmic (arrowheads) localization. Scale bars, 40 μm.

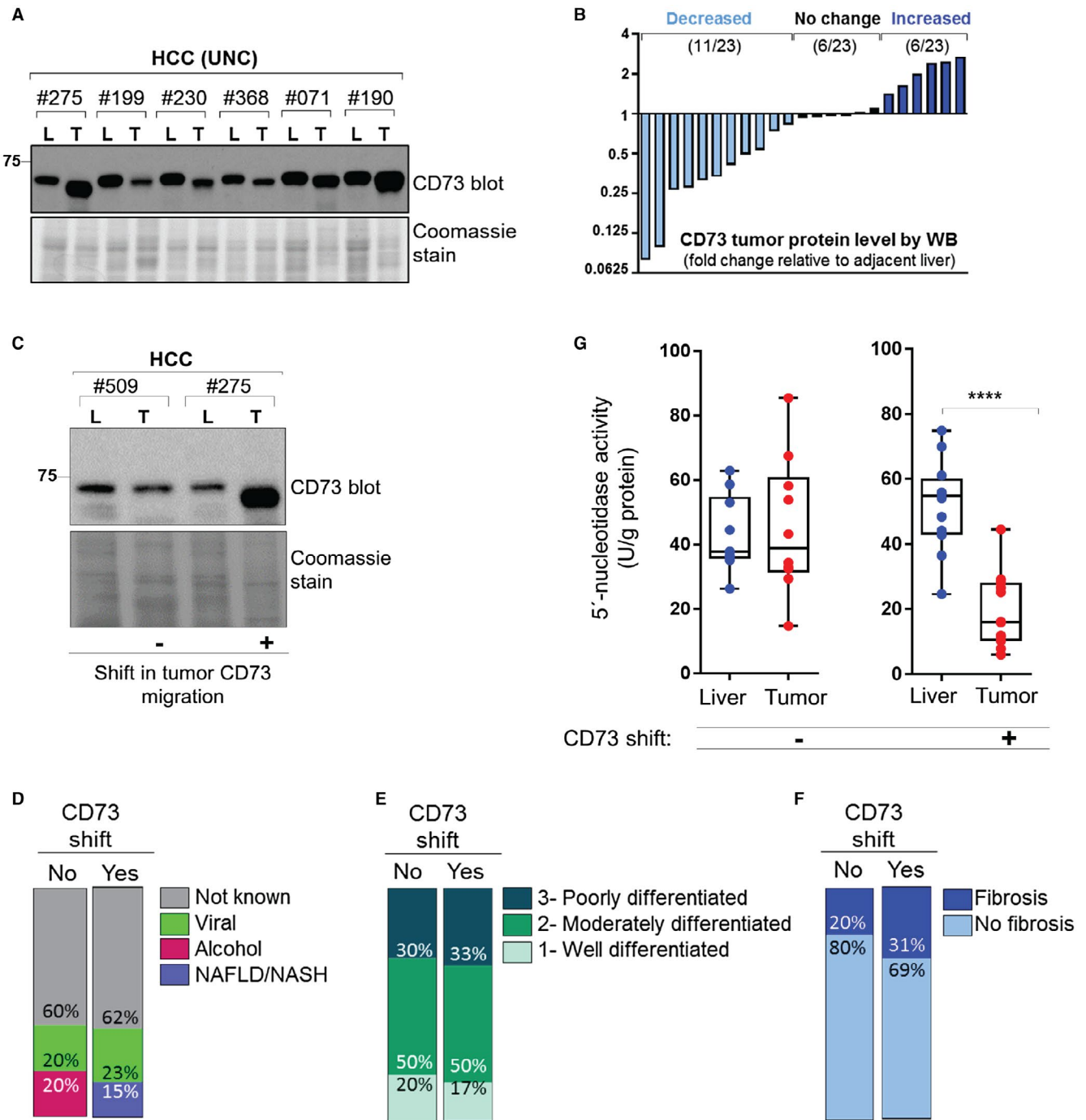


**FIG. 3.** HCC tumor-specific CD73 biochemical alterations correlate with decreased 5'-nucleotidase activity. (A) Representative immunoblot (top) of CD73 in adjacent liver and tumor OG lysates from surgical HCC specimens collected at UNC. Coomassie-stained gel serves as a loading control. The numbers represent individual patients. (B) Densitometric quantification of CD73 protein from immunoblot analysis of 23 pairs of adjacent liver and tumor tissues from patients with HCC. (C) Representative CD73 immunoblots of HCC adjacent liver and tumor tissue OG lysates from 2 patients, demonstrating differences in tumor CD73 migration on SDS-PAGE. (D-F) Distribution of (D) HCC etiology, (E) tumor stage, and (F) fibrosis status across tumor samples without CD73 shift (left bars; n = 10) and with CD73 shift (right bars; n = 12-13). Clinical and biochemical data on all samples are provided in Supporting File S1. (G) Measurement of 5'-nucleotidase activity in adjacent liver and tumor tissue OG lysates from HCC cases in which tumor CD73 did not exhibit a shift in migration (left panel; cases similar to #509 in C) and in HCC cases where there was a significant shift (right panel; cases similar to #275 in C). Box and whiskers plot. \*\*\*\**P* < 0.0001; paired *t* test. Abbreviations: L, adjacent liver tissue; NAFLD, nonalcoholic fatty liver disease; NASH, nonalcoholic steatohepatitis; T, tumor tissue; WB, western blot.



presence of fibrosis (Fig. 3D-F). However, altered biochemical processing of CD73 in the HCC tumors was associated with significantly decreased enzymatic activity (Fig. 3G). Although there was a negative correlation trend between CD73 shift with disease-free status ( $P = 0.20$ ) and patient survival ( $P = 0.28$ ), it was not statistically significant (Supporting Fig. S1A-C). Similarly, total tumor CD73 expression did not correlate with clinical outcomes based on the samples tested here (Supporting Fig. S1D-F).

## CD73 UNDERGOES DIFFERENTIAL GLYCOSYLATION IN HCC TUMORS RELATIVE TO ADJACENT NONTUMOR TISSUE

CD73 has four consensus *N*-glycosylation motifs: <sup>53</sup>NAS, <sup>311</sup>NSS, <sup>333</sup>NYS, and <sup>403</sup>NGT (Fig. 4A). Changes in glycosylation at one or more of these sites may alter CD73 activity because three (N311/N333/N403) are located in the C-terminal catalytic domain of the molecule.<sup>(19)</sup> Therefore, we tested the hypothesis that tumor CD73 undergoes altered glycosylation. To that end, we deglycosylated CD73 *in vitro* using EndoH (typically removes immature high mannose glycans introduced in the ER) and PNGase F (removes more mature complex glycans introduced post-ER exit). The differential migration on the gel was not present after PNGase F treatment but was still present in the EndoH-resistant fraction (Fig. 4B). This suggested that glycosylation differences on tumor CD73 are introduced after exit from the ER. MS glycomics analysis revealed that the majority of CD73 glycans are conjugated to N311 and N333, followed by N403 and N53 (Fig. 4C). While N333 was conjugated primarily to complex glycans, N311 displayed a mix of high mannose, hybrid, and complex glycans (Fig. 4D). Globally, the major glycosylation differences on CD73 from HCC tumors were in specific glycan structures, with a significant increase in high mannose glycans and a decrease in hybrid glycans (Fig. 5A). The greatest glycosylation changes were observed at site N311 (Fig. 5B), where under normal conditions high mannose glycans accounted for <20% of all glycans; in tumor CD73, this residue was highly mannosylated (>60% of total glycans). In addition, incorporation of complex glycans was significantly reduced at both the N311 and N333 sites (Fig. 5B,C).

## SITE-SPECIFIC GLYCOSYLATION REGULATES CD73 ENZYMATIC ACTIVITY AND SUBCELLULAR DISTRIBUTION

To assess the functional significance of site-specific CD73 *N*-glycosylation, we generated nonglycosylatable mutants (N311Q and N333Q) and compared their enzymatic activity to wild-type (WT) CD73 (Fig. 5D). The glycosylation-deficient N311Q and N333Q mutants had 30% and 50% lower enzyme activity, respectively, compared to WT CD73. Furthermore, the subcellular distribution of both mutants appeared predominantly perinuclear compared to WT CD73 (Fig. 5E). To assess whether the intracellular CD73 puncta colocalize with the Golgi organelle, where most of the hybrid and complex glycans are conjugated to proteins, we costained with the Golgi marker GM130. The glycosylation-deficient and catalytically-impaired N333Q mutant partially colocalized with GM130 (Fig. 5F), suggesting that it is partly retained in the Golgi compartment. Combined, these data demonstrate that *N*-glycosylation of CD73 at N311 and N333, the two sites that are aberrantly glycosylated on CD73 in primary HCC tumors, is important for CD73 function.

## UP-REGULATION OF GOLGI PROTEIN GM130 AND GLOBAL DIFFERENCES IN THE EXPRESSION OF GENES ENCODING *N*-LINKED GLYCOPROTEINS IN HCC TUMORS

We analyzed major proteins that regulate the transit of GPI-APs through the Golgi organelle, including GM130, which is important for glycosylation and maintenance of Golgi structure; the *v*-SNARE (Vti1) and *t*-SNARE (syntaxin-6) proteins involved in vesicle transport through the Golgi, and a SNAP receptor that regulates protein transport in the Golgi (GS27). GM130 exhibited the most profound differences between tumor and adjacent nontumor tissue and was up-regulated more than 8-fold in HCC tumors (Fig. 6A,B). While in adjacent nontumor human liver tissue, GM130 staining appeared as perinuclear puncta; in HCC tumors, the puncta appeared enlarged and merged, forming larger structures (Fig. 6C).



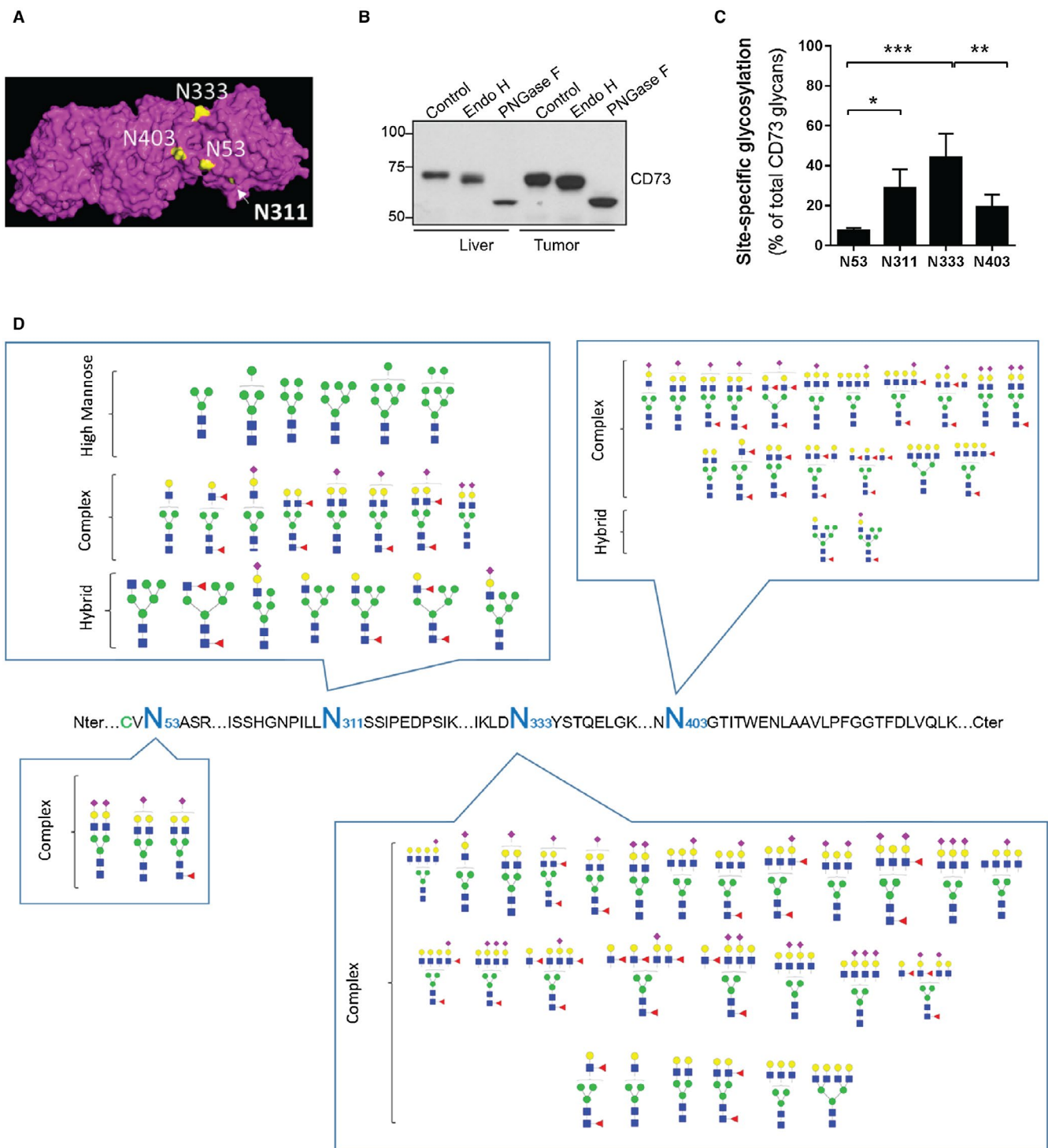


**FIG. 4.** Site-specific glycan distribution on CD73 in normal human liver. (A) Model of CD73 dimer structure (magenta) showing the four asparagine residues (yellow) that are targets of glycosylation. Structure of CD73 dimer was generated using Pymol (PDB: 4H1S). (B) Effect of *in vitro* CD73 deglycosylation using PNGase F or EndoH. (C) Relative abundance of glycans across the four CD73 N-linked glycosylation sites, demonstrating that N311 and N333 account for >70% of all glycans. Bars represent mean  $\pm$  SD. \* $P < 0.05$ ; \*\* $P < 0.01$ ; \*\*\* $P < 0.001$ ; one-way ANOVA Tukey's multiple comparisons test. (D) Types of glycans present on the four CD73 glycosylation sites. GlcNAc (■), mannose (●), fucose (◄), galactose (●), Neu5Ac (◆).

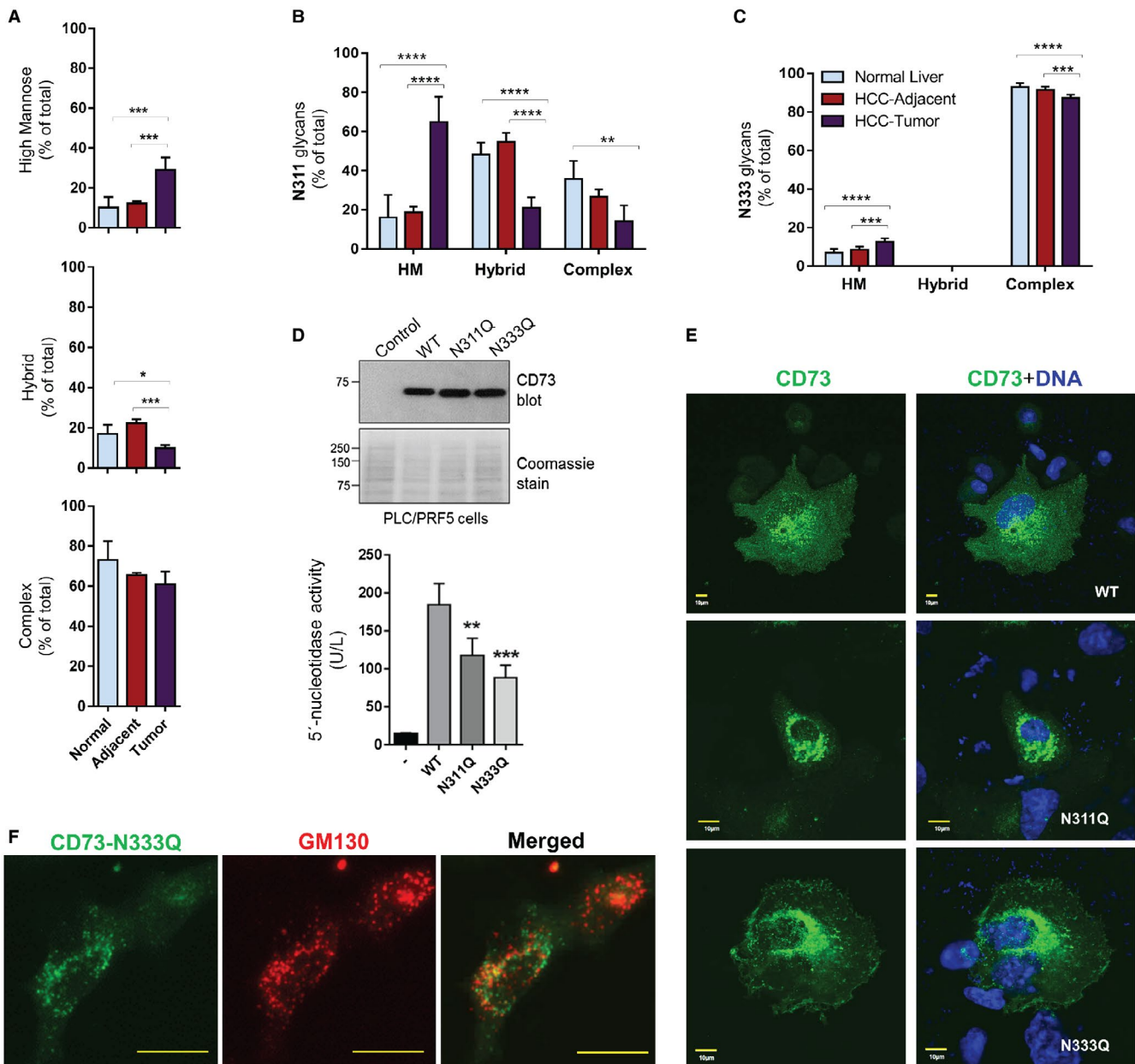


**FIG. 5.** Site-specific increase in high mannose glycans promotes CD73 intracellular retention and decreased enzymatic activity. (A) Percent of high mannose (top), hybrid (middle), and complex (bottom) glycans on CD73 extracted from normal liver tissue (non-HCC;  $n = 4$ ), HCC adjacent liver tissue ( $n = 5$ ), and HCC tumor tissue ( $n = 5$ ). Bars represent mean  $\pm$  SD.  $*P < 0.05$ ;  $***P < 0.001$ ; one-way ANOVA. (B,C) Changes in glycan composition on the two major CD73 glycosylation sites, N311 and N333.  $**P < 0.01$ ;  $***P < 0.001$ ;  $****P < 0.0001$ . Bars represent mean  $\pm$  SD. (D) Representative CD73 immunoblot (top) of PLC/PRF5 cells transfected with empty vector, WT CD73, and glycosylation mutants N311Q and N333Q, demonstrating equal overexpression of CD73 protein. Measurement of 5'-nucleotidase activity (bottom) in lysates of control vector-transfected (-) or CD73-transfected PLC/PRF5 cells ( $n = 3$ ). Data are representative of at least three independent experiments. Bars represent mean  $\pm$  SD.  $**P < 0.01$ ;  $***P < 0.001$ ; one-way ANOVA. (E) Subcellular distribution of WT and glycosylation point mutant CD73 transfected in PLC/PRF5 cells. Green, CD73; blue, DNA. Scale bars, 10  $\mu$ m. (F) Colocalization between CD73-N333Q (green) and the Golgi marker protein GM130 (red). Scale bar, 20  $\mu$ m. Abbreviation: HM, high mannose.

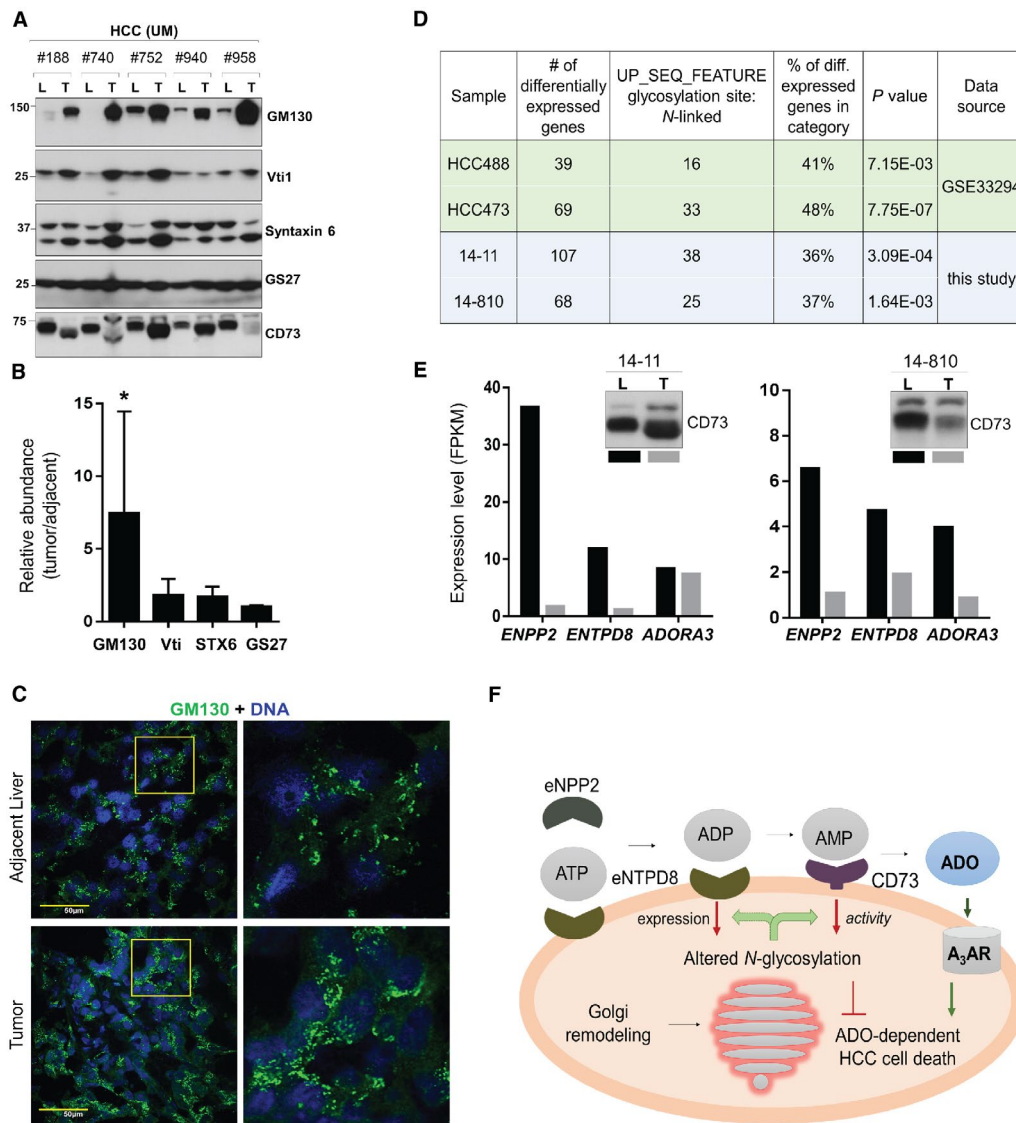


**FIG. 6.** Increased expression of the Golgi protein GM130 in HCC tumors correlates with global expression changes in *N*-linked glycoprotein-encoding genes. (A) Immunoblot of Golgi-resident proteins GM130, Vti1, syntaxin 6, and GS27 in HCC adjacent liver and tumor lysates. (B) Quantification of the immunoblots in panel A. Bars represent mean  $\pm$  SD. \* $P < 0.05$  compared to GS27; one-way ANOVA; Tukey's multiple comparisons test. (C) Double immunofluorescence staining of GM130 (green) and DNA (blue) in adjacent liver and tumor tissue (representative images are from HCC case #752). Scale bars, 50  $\mu$ m. Right panels show the respective magnified areas (represented by the yellow boxes). (D) RNAseq analysis on four pairs of HCC adjacent liver–tumor pairs revealing the percentage (36%–48%) of significantly differentially expressed genes that encode *N*-linked glycoproteins (complete data set is in Supporting File S2). (E) RNA expression levels of select *N*-linked glycoprotein genes (*eNPP2*, *eENTPD8*, and *ADORA3*) in paired HCC adjacent liver (black bars) and tumor tissues (gray bars). Each bar represents a single readout from the RNAseq data set (Supporting File S2). (F) Summary of findings and working hypothesis model of HCC tumor-specific changes in *N*-glycosylation. HCC tumors exhibit altered Golgi structure, as exemplified by significant overexpression of the structural protein GM130. Changes in Golgi structure lead to altered localization and decreased function of *N*-linked glycoproteins, including ecto-nucleotidase CD73, and are associated with decreased expression of *eNPP2* and *eENTPD8*, leading to overall decreased levels in the production of extracellular adenosine. Decreased adenosine production by the highly mannoseylated tumor CD73 blunts adenosine-dependent HCC cell death by the A<sub>3</sub> adenosine receptor, promoting HCC progression. Abbreviations: A<sub>3</sub>AR, A<sub>3</sub> adenosine receptor; ADO, adenosine; *ADORA3*, adenosine A<sub>3</sub> receptor gene; ADP, adenosine diphosphate; ATP, adenosine triphosphate; *eNPP2*, ectonucleotide pyrophosphatase/phosphodiesterase 2 gene; FPKM, fragments per kilobase of exon model per million reads mapped; L, adjacent liver tissue; T, tumor tissue.



RNA sequencing (RNAseq) analysis was performed on two pairs of HCC specimens (adjacent tissue and tumor tissue) that displayed differences in CD73 migration on gel, as shown in insets to Fig. 6E. We additionally analyzed gene expression data on two HCC liver-tumor pairs from a published RNAseq data set (GSE 33294). These results revealed that *N*-linked glycoprotein-encoding genes were among the most represented category of differentially expressed genes (Fig. 6D; Supporting File S2). Because ecto-nucleotidases that act upstream of CD73 in the liver (e.g., ectonucleotide pyrophosphatase/phosphodiesterase 2 [eNPP2] and ectonucleoside triphosphate diphosphohydrolase 8 [eNTPD8]),<sup>(27)</sup> as well as the A<sub>3</sub>AR are also *N*-glycosylated, we compared their gene expression levels in nontumor versus tumor tissue from the RNAseq sets. This comparison revealed a general decrease in expression (11%-95%) in the tumors compared to adjacent liver tissue (Fig. 6E). Taking into account the RNAseq results and the molecular and biochemical studies, we propose a model for a tumor-selective mechanism to limit extracellular adenosine signaling in HCC tumors by (i) disruption of CD73 glycosylation leading to decreased activity and (ii) transcriptional down-regulation of ecto-nucleotidases supplying the AMP substrate of CD73, such as eNTPD8 (Fig. 6F).

## Discussion

### CD73 AS A POTENTIAL TARGET IN HCC

HCC accounts for the vast majority of primary liver cancer cases, and there are ~850,000 new cases diagnosed worldwide each year.<sup>(28)</sup> While death rates continue to decline for most cancer types, recent trends in the United States reveal that liver cancer mortality has continued to increase at a rate of 2.5%-3% per year and 5-year survival remains below 20%.<sup>(29)</sup> At the onset of symptoms, HCC is typically advanced and not amenable to current treatment approaches, which are very limited. Direct modulation of adenosine receptor activity represents a promising therapeutic strategy for patients with HCC.<sup>(17)</sup> In addition to direct-acting agonists, such as the clinical candidate A<sub>3</sub>AR agonist CF102,

an alternative approach is to augment the generation of the endogenous ligand adenosine. Here, we demonstrate that the adenosine-generating function of CD73 is compromised in human HCC tumors due to aberrant *N*-linked glycosylation. Aside from revealing a novel mechanism in HCC tumor biology, our results may potentially help to identify patients who are more likely to benefit from A<sub>3</sub>AR agonists based on their tumor CD73 glycosylation status, localization, and activity. While our primary focus here was on tumor hepatocytes and HCC cells, the regulation and function of CD73 on other cell types, such as endothelial cells and lymphocytes, will need to be taken into account in future studies to determine if CD73 augmentation or blockade could be of potential benefit to patients with HCC.

### DIFFERENCES IN CD73 REGULATION AND FUNCTION ACROSS CANCER TYPES

Tumor-selective transcriptional up-regulation of *NT5E* can be protumorigenic as high expression of epithelial CD73 is associated with low levels of tumor-infiltrating leukocytes and reduced disease-free and overall survival in triple-negative breast cancer.<sup>(30)</sup> However, in contrast to breast cancer, CD73 is significantly down-regulated in advanced endometrial tumors compared to normal endometrium and less aggressive tumors,<sup>(6,9)</sup> similar to invasive bladder cancer,<sup>(31,32)</sup> in both cases high expression predicts more favorable patient outcome. In the case of endometrial cancer, down-regulation of CD73 is detrimental as it leads to compromised integrity of the epithelial barrier. Specifically, CD73-generated adenosine is necessary for A<sub>1</sub>AR receptor-dependent cortical actin polymerization and cell-cell adhesion.<sup>(9)</sup> Our results herein reveal that posttranslational modulation of the CD73 nucleotidase function by *N*-linked glycosylation is yet another important but underappreciated mechanism for modulating CD73 function. Given our findings, assessment of CD73 expression by tissue staining alone does not necessarily reflect presence of the active enzyme as more detailed biochemical studies are needed to probe that function. Resolving which mode of CD73 regulation is most relevant for the specific tumor type will aid in understanding which patients are likely to benefit from CD73 blocking antibodies.

## THE NEED FOR ROBUST PRECLINICAL *IN VIVO* STUDIES ON THE ROLE OF CD73 IN HCC

Studies examining how CD73 loss impacts HCC development in rodent models have not been performed, with the exception of a limited analysis reporting that subcutaneous inoculation of MHCC97-derived tumors showed decreased growth in CD73<sup>-/-</sup> compared to WT mice.<sup>(33)</sup> Use of global and tissue-specific CD73 knockout models in combination with standard HCC induction models, such as chemical carcinogenesis, fatty liver disease, and alcohol-induced liver disease,<sup>(34)</sup> will help address this question in a rigorous manner in future studies. One major caveat is that CD73 regulation in humans is different from rodents, as we have shown to be the case with the posttranscriptional processing of the *NT5E* gene, which is uniquely spliced in humans compared to all other species.<sup>(22)</sup> Therefore, the use of humanized mice and patient-derived xenograft mouse models will likely be warranted.

## POSTTRANSCRIPTIONAL AND POSTTRANSLATIONAL REGULATION MECHANISMS ALTER CD73 FUNCTIONS

Our prior and current results demonstrate that the major mechanism of CD73 regulation in HCC is not transcriptional but posttranscriptional<sup>(22)</sup> and posttranslational (current study). Previously, we demonstrated that alternative splicing generates a novel human-specific CD73 isoform in cirrhosis and HCC (CD73S) that is present in both adjacent nontumor tissue and tumor tissue and acts in a dominant-negative fashion.<sup>(22)</sup> Our current results provide additional evidence that the activity of the major canonical CD73 protein is selectively altered by *N*-linked glycosylation to produce a highly mannosylated and enzymatically impaired glycoform in HCC tumors. Understanding the pathways that lead to these changes may reveal additional molecular targets to elevate CD73 activity selectively in HCC tumors. For example, restoration of Golgi morphology and glycosylation has been shown to enhance the susceptibility of prostate cancer cells to apoptosis,<sup>(35)</sup> and similar approaches may be explored in HCC. Our results may also help explain several previously reported functions of

CD73 in multiple cell types that are independent of its activity as an AMPase, such as T-cell activation by protein-protein interactions to deliver a costimulatory signal,<sup>(36)</sup> promoting adhesion of lymphocytes to the endothelium,<sup>(37)</sup> conferring resistance to apoptosis of leukemia cells,<sup>(38)</sup> and inducing phosphorylation of intracellular proteins in response to antibody ligation.<sup>(39,40)</sup> Therefore, it is plausible that *N*-linked glycosylation is a mechanism to tune adenosine-independent CD73 functions in different cell types under physiological and disease states.

## CD73 AS A MARKER OF GOLGI ORGANELLE DYSFUNCTION IN HCC TUMORS

The significant and selective up-regulation of GM130 in HCC tumors implicates the Golgi organelle in HCC tumor biology. The Golgi apparatus is the central compartment of the secretory pathway where proteins and lipids are extensively modified as they traverse the organelle en route to their intended destination to cellular membranes or to being secreted outside the cell. Proper architecture of the Golgi, which is composed of stacks of cisternae, ensures that the various enzymes involved in the modification of proteins and lipids are localized to their proper compartment. The Golgi structural protein GM130 is critical for the lateral linking of Golgi elements, which in turn ensures the proper localization of glycosylation enzymes.<sup>(41)</sup> It was shown that down-regulation of GM130 had antitumor effects in a mouse model of lung cancer.<sup>(42)</sup> Presently, it is not clear what causes the Golgi alterations in cancer, but it is known that many genes, in particular kinases, exert control of this important organelle.<sup>(43)</sup> Therefore, the mechanism behind up-regulated GM130 expression in HCC tumors remains to be investigated and may involve kinome-level changes.

## *N*-LINKED GLYCOSYLATION AS A MECHANISM FOR HCC PROGRESSION

Previous studies aimed at identifying serum biomarkers reported major HCC-associated alterations in the types and abundance of glycans on specific serum proteins, such as  $\alpha$ -fetoprotein and Golgi protein 73.<sup>(44-47)</sup> Aside from being a biomarker of

HCC, altered *N*-glycosylation can also serve a functional role to promote HCC tumor metastasis. For example, altered *N*-glycan branching of CD147 enhances its binding to  $\beta$ 1-integrin to promote HCC tumor metastasis.<sup>(48)</sup> While the functional significance of elevated high-mannose glycans that we identified on HCC tumor CD73 is not clear, global high mannose glycosylation negatively affects multiple essential functions of the intestinal epithelium, such as permeability, host-microbe interactions, and the activities of membrane-associated proteins.<sup>(49)</sup> Therefore, it is plausible that the highly mannosylated CD73 tumor glycoform blocks the tissue barrier function of CD73.<sup>(6)</sup> This will be a key question for future studies.

## REFERENCES

- Zimmermann H, Zebisch M, Strater N. Cellular function and molecular structure of ecto-nucleotidases. *Purinergic Signal* 2012;8:437-502.
- Ipata PL, Balestri F. The functional logic of cytosolic 5'-nucleotidases. *Curr Med Chem* 2013;20:4205-4216.
- Antonoli L, Yegutkin GG, Pacher P, Blandizzi C, Hasko G. Anti-CD73 in cancer immunotherapy: awakening new opportunities. *Trends Cancer* 2016;2:95-109.
- Hay CM, Sult E, Huang Q, Mulgrew K, Fuhrmann SR, McGlinchey KA, et al. Targeting CD73 in the tumor microenvironment with MEDI9447. *Oncoimmunology* 2016; 5:e1208875.
- Perrot I, Michaud HA**, Giraudon-Paoli M, Augier S, Docquier A, Gros L, et al. Blocking antibodies targeting the CD39/CD73 immunosuppressive pathway unleash immune responses in combination cancer therapies. *Cell Rep* 2019;27:2411-2425. e2419.
- Bowser JL, Broaddus RR. CD73s protection of epithelial integrity: thinking beyond the barrier. *Tissue Barriers* 2016;4: e1224963.
- Synnestvedt K, Furuta GT, Comerford KM, Louis N, Karhausen J, Eltzschig HK, et al. Ecto-5'-nucleotidase (CD73) regulation by hypoxia-inducible factor-1 mediates permeability changes in intestinal epithelia. *J Clin Invest* 2002;110:993-1002.
- Thompson LF, Eltzschig HK, Ibla JC, Van De Wiele CJ, Resta R, Morote-Garcia JC, et al. Crucial role for ecto-5'-nucleotidase (CD73) in vascular leakage during hypoxia. *J Exp Med* 2004;200:1395-1405.
- Bowser JL, Blackburn MR, Shipley GL, Molina JG, Dunner K Jr, Broaddus RR. Loss of CD73-mediated actin polymerization promotes endometrial tumor progression. *J Clin Invest* 2016;126:220-238.
- Hart ML, Much C, Gorzolla IC, Schittenhelm J, Kloor D, Stahl GL, et al. Extracellular adenosine production by ecto-5'-nucleotidase protects during murine hepatic ischemic preconditioning. *Gastroenterology* 2008;135:1739-1750.e1733.
- Snider NT, Griggs NW, Singla A, Moons DS, Weerasinghe SV, Lok AS, et al. CD73 (ecto-5'-nucleotidase) hepatocyte levels differ across mouse strains and contribute to mallory-denk body formation. *Hepatology* 2013;58:1790-1800.
- Peng Z, Fernandez P, Wilder T, Yee H, Chiriboga L, Chan ES, et al. Ecto-5'-nucleotidase (CD73) -mediated extracellular adenosine production plays a critical role in hepatic fibrosis. *FASEB J* 2008;22:2263-2272.
- Fausther M, Sheung N, Saiman Y, Bansal MB, Dranoff JA. Activated hepatic stellate cells upregulate transcription of ecto-5'-nucleotidase/CD73 via specific SP1 and SMAD promoter elements. *Am J Physiol Gastrointest Liver Physiol* 2012;303:G904-G914.
- Global Burden of Disease Liver Cancer Collaboration, Akinyemiju T, Abera S, Ahmed M, Alam N, Alemayohu MA, et al. to 2015 at the global, regional, and national level: results from the Global Burden of Disease Study 2015. *JAMA Oncol* 1990;2017(3):1683-1691.
- Sciarra A, Monteiro I, Menetrier-Caux C, Caux C, Gilbert B, Halkic N, et al. CD73 expression in normal and pathological human hepatobiliarypancreatic tissues. *Cancer Immunol Immunother* 2019;68:467-478. Erratum in: *Cancer Immunol Immunother* 2019;68:529.
- Cohen S, Stemmer SM, Zozulya G, Ochaion A, Patoka R, Barer F, et al. CF102 an A3 adenosine receptor agonist mediates anti-tumor and anti-inflammatory effects in the liver. *J Cell Physiol* 2011;226:2438-2447.
- Stemmer SM, Benjaminov O, Medalia G, Ciuraru NB, Silverman MH, Bar-Yehuda S, et al. CF102 for the treatment of hepatocellular carcinoma: a phase I/II, open-label, dose-escalation study. *Oncologist* 2013;18:25-26.
- Stemmer SM, Manojlovic NS, Marinca MV, Petrov P, Cherciu N, Ganea D, et al. A phase II, randomized, double-blind, placebo-controlled trial evaluating efficacy and safety of namodenoson (CF102), an A3 adenosine receptor agonist (A3AR), as a second-line treatment in patients with Child-Pugh B (CPB) advanced hepatocellular carcinoma (HCC). *J Clin Oncol* 2019; 37:2503-2503.
- Knapp K, Zebisch M, Pippel J, El-Tayeb A, Muller CE, Strater N. Crystal structure of the human ecto-5'-nucleotidase (CD73): insights into the regulation of purinergic signaling. *Structure* 2012;20:2161-2173.
- Moremen KW, Tiemeyer M, Nairn AV. Vertebrate protein glycosylation: diversity, synthesis and function. *Nat Rev Mol Cell Biol* 2012;13:448-462.
- Stowell SR, Ju T, Cummings RD. Protein glycosylation in cancer. *Annu Rev Pathol* 2015;10:473-510.
- Snider NT, Altschuler PJ, Wan S, Welling TH, Cavalcoli J, Omary MB. Alternative splicing of human NT5E in cirrhosis and hepatocellular carcinoma produces a negative regulator of ecto-5'-nucleotidase (CD73). *Mol Biol Cell* 2014;25:4024-4033.
- Strum JS, Nwosu CC, Hua S, Kronewitter SR, Seipert RR, Bachelor RJ, et al. Automated assignments of N- and O-site specific glycosylation with extensive glycan heterogeneity of glycoprotein mixtures. *Anal Chem* 2013;85:5666-5675.
- Tsou CC, Avtonomov D, Larsen B, Tucholska M, Choi H, Gingras AC, et al. DIA-Umpire: comprehensive computational framework for data-independent acquisition proteomics. *Nat Methods* 2015;12:258-264.
- Thorsson V, Gibbs DL, Brown SD, Wolf D, Bortone DS, Ou Yang TH, et al. Cancer Genome Atlas Research Network. The immune landscape of cancer. *Immunity* 2018;48:812-830.e814.
- Chiu JH, Hu CP, Lui WY, Lo SC, Chang CM. The formation of bile canaliculi in human hepatoma cell lines. *Hepatology* 1990;11:834-842.
- Fausther M, Lecka J, Soliman E, Kauffenstein G, Pelletier J, Sheung N, et al. Coexpression of ecto-5'-nucleotidase/CD73 with specific NTPDases differentially regulates adenosine formation in the rat liver. *Am J Physiol Gastrointest Liver Physiol* 2012;302:G447-G459.



- 28) Llovet JM, Zucman-Rossi J, Pikarsky E, Sangro B, Schwartz M, Sherman M, et al. Hepatocellular carcinoma. *Nat Rev Dis Primers* 2016;2:16018.
- 29) Jemal A, Ward EM, Johnson CJ, Cronin KA, Ma J, Ryerson B, et al. Annual report to the nation on the status of cancer, 1975-2014, featuring survival. *J Natl Cancer Inst* 2017;109:1975-2014.
- 30) Buisseret L, Pommey S, Allard B, Garaud S, Bergeron M, Cousineau I, et al. Clinical significance of CD73 in triple-negative breast cancer: multiplex analysis of a phase III clinical trial. *Ann Oncol* 2018;29:1056-1062.
- 31) Wettstein MS, Buser L, Hermanns T, Roudnický F, Eberli D, Baumeister P, et al. CD73 predicts favorable prognosis in patients with nonmuscle-invasive urothelial bladder cancer. *Dis Markers* 2015;2015:785461.
- 32) Koivisto MK, Tervahartiala M, Kenessey I, Jalkanen S, Bostrom PJ, Salmi M. Cell-type-specific CD73 expression is an independent prognostic factor in bladder cancer. *Carcinogenesis* 2019;40:84-92.
- 33) Shali S, Yu J, Zhang X, Wang X, Jin Y, Su M, et al. Ecto-5'-nucleotidase (CD73) is a potential target of hepatocellular carcinoma. *J Cell Physiol* 2019;234:10248-10259.
- 34) Brown ZJ, Heinrich B, Greten TF. Mouse models of hepatocellular carcinoma: an overview and highlights for immunotherapy research. *Nat Rev Gastroenterol Hepatol* 2018;15:536-554.
- 35) Petrosyan A, Holzapfel MS, Muirhead DE, Cheng PW. Restoration of compact Golgi morphology in advanced prostate cancer enhances susceptibility to galectin-1-induced apoptosis by modifying mucin O-glycan synthesis. *Mol Cancer Res* 2014;12:1704-1716.
- 36) Resta R, Thompson LF. T cell signalling through CD73. *Cell Signal* 1997;9:131-139.
- 37) Airas L, Hellman J, Salmi M, Bono P, Puurunen T, Smith DJ, et al. CD73 is involved in lymphocyte binding to the endothelium: characterization of lymphocyte-vascular adhesion protein 2 identifies it as CD73. *J Exp Med* 1995;182:1603-1608.
- 38) Mikhailov A, Sokolovskaya A, Yegutkin GG, Amdahl H, West A, Yagita H, et al. CD73 participates in cellular multiresistance program and protects against TRAIL-induced apoptosis. *J Immunol* 2008;181:464-475.
- 39) Airas L, Niemela J, Salmi M, Puurunen T, Smith DJ, Jalkanen S. Differential regulation and function of CD73, a glycosylphosphatidylinositol-linked 70-kD adhesion molecule, on lymphocytes and endothelial cells. *J Cell Biol* 1997;136:421-431.
- 40) Dianzani U, Redoglia V, Bragardo M, Attisano C, Bianchi A, Di Franco D, et al. Co-stimulatory signal delivered by CD73 molecule to human CD45RAhiCD45ROlo (naive) CD8+ T lymphocytes. *J Immunol* 1993;151:3961-3970.
- 41) Puthenveedu MA, Bachert C, Puri S, Lanni F, Linstedt AD. GM130 and GRASP65-dependent lateral cisternal fusion allows uniform Golgi-enzyme distribution. *Nat Cell Biol* 2006;8:238-248.
- 42) Chang SH, Hong SH, Jiang HL, Minai-Tehrani A, Yu KN, Lee JH, et al. GOLGA2/GM130, cis-Golgi matrix protein, is a novel target of anticancer gene therapy. *Mol Ther* 2012;20:2052-2063.
- 43) Chia J, Goh G, Racine V, Ng S, Kumar P, Bard F. RNAi screening reveals a large signaling network controlling the Golgi apparatus in human cells. *Mol Syst Biol* 2012;8:629.
- 44) Mehta A, Herrera H, Block T. Glycosylation and liver cancer. *Adv Cancer Res* 2015;126:257-279.
- 45) Kim H, Kim K, Jin J, Park J, Yu SJ, Yoon JH, et al. Measurement of glycosylated alpha-fetoprotein improves diagnostic power over the native form in hepatocellular carcinoma. *PLoS One* 2014;9:e110366.
- 46) Jiang K, Li W, Zhang Q, Yan G, Guo K, Zhang S, et al. GP73 N-glycosylation at Asn144 reduces hepatocellular carcinoma cell motility and invasiveness. *Oncotarget* 2016;7:23530-23541.
- 47) Norton PA, Comunale MA, Krakover J, Rodemich L, Pirog N, D'Amelio A, et al. N-linked glycosylation of the liver cancer biomarker GP73. *J Cell Biochem* 2008;104:136-149.
- 48) **Cui J, Huang W, Wu B**, Jin J, Jing L, Shi WP, et al. N-glycosylation by N-acetylglucosaminyltransferase V enhances the interaction of CD147/basigin with integrin beta1 and promotes HCC metastasis. *J Pathol* 2018;245:41-52.
- 49) **Park D, Xu G**, Barboza M, Shah IM, Wong M, Raybould H, et al. Enterocyte glycosylation is responsive to changes in extracellular conditions: implications for membrane functions. *Glycobiology* 2017;27:847-860.

Author names in bold designate shared co-first authorship.

## Supporting Information

Additional Supporting Information may be found at [onlinelibrary.wiley.com/doi/10.1002/hep4.1410/supinfo](http://onlinelibrary.wiley.com/doi/10.1002/hep4.1410/supinfo).